

Politecnico di Torino

Motor Power Consumption Analyzer
Technical Report

Haoyi Chen
Qifan Wu
Yiang Li

Professor: Vincenzo Randazzo

01NOKOQ - Electronic systems engineering
Politecnico di Torino
November 2026

Contents

1 Introduction **1**

1.1 Project Specification 1

1.2 Design Flow 2

2 System Overview **4**

3 Hardware Design **5**

3.1 Component Selection 5

3.1.1 Current and Power Monitor: INA226 5

3.1.2 Microcontroller and BLE SoC: CC2640R2F 7

3.1.3 Current Sensing Resistor and Input Protection 8

3.1.4 Power Supply Components 10

3.1.5 Isolation Components 12

3.2 Schematic Design 14

3.3 Layout Design 18

3.3.1 4-Layer Stack-up and Layer Assignment 18

3.3.2 Functional Zoning and Sub-system Distribution 19

4 Manufacturing and DFM Validation **22**

5 Hardware Testing **23**

6 Software Design **25**

6.1 Firmware Architecture 25

6.2 Software Logic 25

6.3 Mobile Application Interface 27

7 Full Functional Validation **28**

7.1 System-Level Test Result 28

7.2 Fault Analysis and Debugging Process 29

1 Introduction

Motor power consumption monitoring is an important task in embedded motor control and energy analysis applications. During motor operation, the current drawn by the motor can change significantly depending on the load condition, start-up transient, speed variation, and mechanical resistance. Therefore, a dedicated measurement system is required to monitor both the supply voltage and the current flowing through the motor in real time.

The objective of this project is to design a PCB-based motor power consumption analyzer. The system is intended to be connected in series with the motor power path, where the motor current can be measured through a low-value shunt resistor. The voltage drop across the shunt resistor and the motor bus voltage are measured by a current and power monitor. These measured values are then processed by a microcontroller and transmitted wirelessly through Bluetooth Low Energy.

The proposed design uses the INA226 as the main current and power monitoring device. It communicates with the microcontroller through an I^2C interface. Since the motor power side may contain switching noise, ground disturbance, and high current transients, electrical isolation is introduced between the sensing side and the microcontroller side. The isolated communication interface allows the measured data to be transferred safely while keeping the two ground domains separated.

The wireless communication and system control are implemented using the CC2640R2F Bluetooth Low Energy microcontroller. The microcontroller configures the INA226, reads the measurement data, calculates or processes the electrical parameters, and sends the results to an external BLE central device. In this way, the system provides a compact and wireless solution for monitoring motor voltage, current, and power consumption.

1.1 Project Specification

This project consists of developing a compact system able to monitor the electrical power consumption of a DC motor and exchange the measured data through a Bluetooth Low Energy interface. The system is designed to measure the motor supply voltage, motor current, and power consumption by using a digital current and power monitoring IC.

The main requirements of the project are listed in the following:

- Measure the DC motor supply voltage up to 36 V.
- Measure the motor current using a shunt-based sensing method.
- Use a 10 mΩ shunt resistor for current sensing.
- Measure the shunt voltage with a theoretical full-scale range of approximately $\pm$81.92 mV.

- Provide electrical isolation between the motor measurement side and the microcontroller/BLE side.
- Acquire or calculate the motor power consumption from the measured voltage and current.
- Transfer measurement data to the microcontroller through an I2C interface.
- Provide Bluetooth Low Energy communication for wireless data transmission.
- Generate stable low-voltage supply rails for the sensing IC, isolation circuit, and microcontroller.
- Use protection and filtering components to reduce the influence of motor noise and transient disturbances.
- Keep the PCB compact and suitable for practical assembly.
- Use components that are well documented and commercially available.

Moreover, some practical constraints must be considered in the real PCB implementation. The maximum measurable current is theoretically determined by the INA226 shunt voltage range and the selected shunt resistor, but the practical current limit also depends on the fuse rating, connector rating, shunt resistor power rating, PCB trace width, and thermal performance. Therefore, these limitations must be verified during the hardware design stage.

1.2 Design Flow

The design flow of the motor power analyzer starts from the definition of the main measurement targets: motor current, bus voltage, and power consumption.

Based on these requirements, the INA226 current and power monitor is selected as the sensing device, and a low-value shunt resistor is used to convert the motor current into a measurable differential voltage. After the sensing method is defined, the power supply and isolation structure are designed. The input power is converted into the required voltage rails for the sensing circuit and the microcontroller circuit. An isolated power supply and an isolated I^2C interface are used to separate the motor measurement side from the digital control side, improving noise immunity and system reliability. Then, the CC2640R2F microcontroller section is designed. The microcontroller communicates with the INA226 through the isolated I^2C bus, reads the measurement data, processes the results, and transmits the motor parameters through Bluetooth Low Energy. Finally, the PCB layout and firmware development are completed. During layout, attention is paid to the high-current path, shunt resistor connection, ground isolation, decoupling capacitors, and RF antenna routing. The firmware is then developed to configure the INA226, acquire measurement data, and send the results through BLE. The overall design flow can be summarized as follows:

1. Define the measurement requirements.

2. Select the sensing device and shunt resistor.
3. Design the schematic.
4. Complete the PCB layout.
5. Develop the firmware for measurement and BLE transmission.
6. Test the motor power analyzer.

2 System Overview

The overall architecture of the motor power analyzer is shown in Figure 1. The system is composed of five main functional blocks: the motor load, the shunt resistor, the INA226 power monitor, the isolation stage, and the CC2640R2F microcontroller with Bluetooth Low Energy communication.

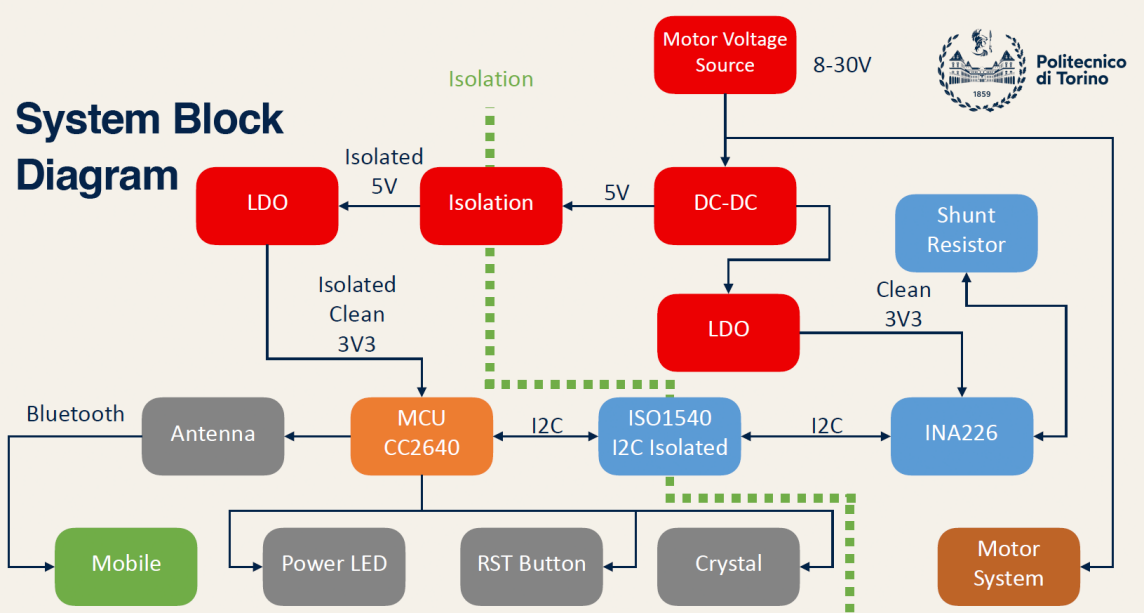


Figure 1: System overview of the motor power consumption analyzer.

As illustrated in the block diagram, the motor system is supplied by an external motor voltage source ranging from 8 V to 30 V. The supply line passes through a shunt resistor, which converts the motor current into a small measurable voltage drop. The INA226 power monitor measures this voltage drop together with the bus voltage, allowing the system to estimate the motor current, voltage, and power consumption during operation.

The sensing side and the microcontroller side are separated by an isolation barrier. On the motor side, a DC–DC converter and a low-dropout regulator provide a clean 3.3 V supply for the INA226. The I2C signals from the INA226 are transferred across the isolation boundary through the ISO1540 isolated I2C interface, which protects the low-voltage control electronics from noise, ground potential differences, and disturbances generated by the motor power stage.

On the isolated control side, a 5 V supply is passed through the isolation stage and regulated by an LDO to generate an isolated clean 3.3 V rail for the CC2640 microcontroller. The microcontroller communicates with the isolated I2C interface, processes the measurement data, and transmits the results wirelessly through the antenna using Bluetooth Low Energy. Additional support components, including the crystal oscillator, reset button, and power LED, provide the basic timing, control, and status indication functions required by the embedded system.

3 Hardware Design

3.1 Component Selection

The component selection of this project was carried out according to the functional requirements of the motor power analyzer. The selected components must support accurate voltage and current measurement, stable power regulation, electrical isolation, embedded data processing, and Bluetooth Low Energy communication.

Each component was chosen based on its role in the system, its electrical characteristics, and its suitability for PCB implementation. The following subsections describe the main devices used in the design and explain the reason for selecting them.

3.1.1 Current and Power Monitor: INA226

The INA226 was selected as the main current and power monitoring IC of the motor power analyzer. It is used to measure the shunt voltage, bus voltage, motor current, and power consumption of the motor supply line. The main electrical parameters considered during the component selection are shown in Figure 2and 3

5.5 Electrical Characteristics

T_A = 25°C, V_{VS} = 3.3 V, V_{IN+} = 12 V, V_{SENSE} = (V_{IN+} – $V_{IN–}$) = 0 mV and V_{VBUS} = 12 V, unless otherwise noted

PARAMETER		TEST CONDITIONS	MIN	TYP	MAX	UNIT
INPUT						
	Shunt voltage input range		–81.9175		81.92	mV
	Bus voltage input range(1)		0		36	V
CMRR	Common-mode rejection	0 V ≤ V_{IN+} ≤ 36 V	126	140		dB
V_{OS}	Shunt offset voltage, RTI(2)			±2.5	±10	µV
	Shunt offset voltage, RTI(2) vs temperature	–40°C ≤ T_A ≤ 125°C		0.02	0.1	µV/°C
PSRR	Shunt offset voltage, RTI(2) vs Power supply	2.7 V ≤ VS ≤ 5.5 V		±2.5		µV/V
V_{OS}	Bus offset voltage, RTI(2)			±1.25	±7.5	mV
	Bus offset voltage, RTI(2) vs temperature	–40°C ≤ T_A ≤ 125°C		10	40	µV/°C
PSRR	Bus offset voltage, RTI(2) vs power supply			±0.5		mV/V
I_B	Input bias current (I_{IN+}, $I_{IN–}$ pins)			0.1		nA
	VBUS input impedance			830		kΩ
	Input leakage (3)	(IN+ pin) + (IN– pin), Power-down mode		0.1	0.5	µA

Figure 2: Relevant electrical characteristics of the INA226.

The main parameters of the INA226 used in this design are listed as follows:

- Bus voltage input range from 0 V to 36 V
- Shunt voltage input range from −81.9175 mV to +81.92 mV
- Supply voltage range from 2.7 V to 5.5 V
- Typical shunt offset voltage of $\pm 2.5, \mu$V
- Maximum shunt offset voltage of $\pm 10, \mu$V

- Typical bus voltage offset of ±1.25 mV
- Maximum bus voltage offset of ±7.5 mV
- VBUS input impedance of approximately 830 kΩ
- I2C and SMBus compatible digital interface
- Programmable conversion time and averaging mode
- Internal calibration register for current and power calculation

POWER SUPPLY					
	Operating supply range		2.7	5.5	V
I_Q	Quiescent current		330	420	µA
	Quiescent current, power-down (shutdown) mode		0.5	2	µA

Figure 3: Supply power of the INA226.

Figure 4 shows the pin assignment of the INA226. The VIN+ and VIN- pins are used to sense the differential voltage across the shunt resistor, while the VBUS pin is connected to the motor supply rail for bus voltage measurement. The SDA and SCL pins provide the I2C/SMBus digital interface to the microcontroller. The A0 and A1 pins are used to configure the I2C address, and the Alert pin can be used for programmable warning or interrupt functions.

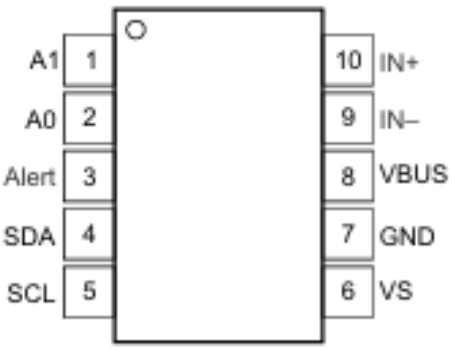


Figure 4: INA226 pin assignment.

In this design, the INA226 measures both the differential shunt voltage and the motor bus voltage. The shunt voltage is defined as

$$V_{\text{shunt}} = V_{\text{IN+}} - V_{\text{IN-}} \tag{1}$$

where $V_{\text{IN+}}$ and $V_{\text{IN-}}$ are the two voltage levels sensed across the shunt resistor. The bus voltage is measured through the **VBUS** pin and represents the motor supply voltage:

$$V_{\text{bus}} = V_{\text{motor}} \tag{2}$$

After obtaining the motor current and bus voltage, the instantaneous electrical power consumed by the motor is calculated as

$$P_{\text{motor}} = V_{\text{bus}} \times I_{\text{motor}} \tag{3}$$

In firmware, the microcontroller periodically reads the INA226 measurement registers through the I^2C interface and converts the raw register values into physical units such as volts, amperes, and watts.

Overall, the INA226 is suitable for this project because it supports high-side current sensing, bus voltage monitoring up to 36 V, digital I2C communication, programmable measurement configuration, and internal current and power calculation. These features reduce the need for external analog circuitry and simplify both the hardware and firmware design of the motor power analyzer.

3.1.2 Microcontroller and BLE SoC: CC2640R2F

The CC2640R2F was selected as the main microcontroller and Bluetooth Low Energy device of the motor power analyzer. It integrates an ARM Cortex-M3 processor and a 2.4 GHz BLE radio in a single chip, which reduces the need for an external Bluetooth module and makes the PCB more compact.

In this project, the CC2640R2F reads the measurement data from the INA226 through the I2C interface, processes the voltage, current, and power values, and transmits the results wirelessly through BLE.

Figure 5 shows the pin assignment of the CC2640R2F package used in the design. The DIO pins can be configured for digital peripherals such as I^2C, UART, SPI, and GPIO. In this project, selected DIO pins are used for the I^2C communication with the INA226 and for system control signals. The `RF_P` and `RF_N` pins are connected to the RF matching network and antenna, while the JTAG pins are used for programming and debugging. The `VDDS`, `VDDR`, and `DCDC` pins are used for the power supply and internal regulation circuit.

The main features considered in this design are listed as follows:

- ARM Cortex-M3 processor core
- Up to 48 MHz clock frequency
- 128 KB programmable Flash memory
- 20 KB ultra-low leakage SRAM
- I2C interface for communication with the INA226
- UART and SPI interfaces for debugging or future expansion

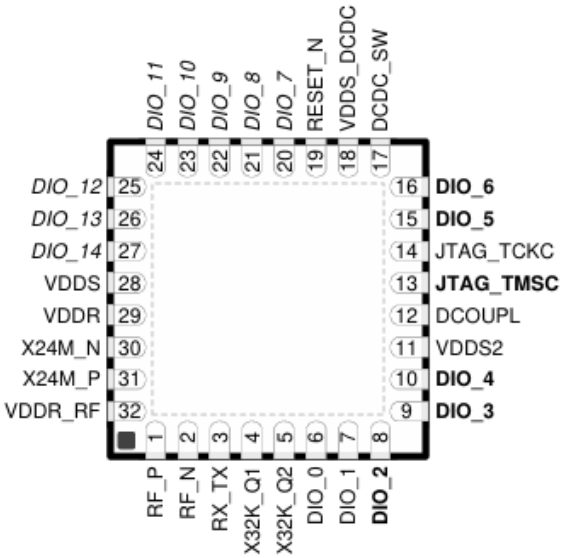


Figure 5: CC2640R2F pin assignment.

- Integrated 2.4 GHz Bluetooth Low Energy radio
- BLE receiver sensitivity of approximately −97 dBm
- Programmable RF output power up to +5 dBm
- Normal operating supply voltage from 1.8 V to 3.8 V
- Low standby and shutdown current
- Compact VQFN package suitable for PCB implementation
- 2-pin cJTAG/JTAG interface for programming and debugging

The CC2640R2F is suitable for this project because it combines embedded control, digital peripheral interfaces, low-power operation, and BLE wireless communication in one device.

3.1.3 Current Sensing Resistor and Input Protection

A low-value current-sense resistor is placed in series with the motor current path. In this design, the selected shunt resistor is 10 mΩ. The voltage drop across this resistor is measured by the INA226 and used to calculate the motor current.

The selected component is the Vishay **WSL3637R0100FEA**, a fixed 10 mΩ Power Metal Strip current-sense resistor. It was selected because it provides low resistance, high power capability, and a 4-terminal structure for accurate Kelvin sensing.

According to Ohm's law, the motor current is calculated from the measured shunt voltage by

$$I_{\text{motor}} = \frac{V_{\text{shunt}}}{R_{\text{shunt}}} \tag{4}$$

In this design, the shunt resistance is

$$R_{\text{shunt}} = 10\ \text{m}\Omega = 0.01\ \Omega \tag{5}$$

Therefore, the current calculation becomes

$$I_{\text{motor}} = \frac{V_{\text{shunt}}}{0.01} \tag{6}$$

For example, if the measured shunt voltage is 10 mV, the corresponding motor current is

$$I_{\text{motor}} = \frac{10\ \text{mV}}{10\ \text{m}\Omega} = 1\ \text{A} \tag{7}$$

The main parameters considered for the selection are listed as follows:

- 4-terminal design for accurate Kelvin sensing
- Selected resistance value: $10\,\text{m}\Omega$
- Power rating of 3 W at 70°C
- Available tolerance of 0.5% or 1.0%
- Temperature coefficient of resistance of ± 50 ppm/°C for $0.003\,\Omega$ to $0.010\,\Omega$
- Operating temperature range from -65°C to $+170$°C
- Very low inductance, from 0.5 nH to 5 nH
- Low thermal EMF, less than $3\,\mu\text{V}/^\circ\text{C}$
- AEC-Q200 qualified for high reliability

The 4-terminal structure is important because the INA226 measures a very small voltage across the shunt resistor. By using Kelvin sensing, the voltage drop caused by high-current PCB traces can be reduced, improving the accuracy of the current measurement.

With the selected $10\,\text{m}\Omega$ resistor and the INA226 shunt voltage range of approximately $\pm 81.92\,\text{mV}$, the theoretical current measurement range is:

$$I_{\text{max}} = \frac{81.92\,\text{mV}}{10\,\text{m}\Omega} \approx 8.19\,\text{A}$$

At this current level, the power dissipated by the shunt resistor is:

$$P_{\text{shunt}} = I^2 R = (8.19\,\text{A})^2 \times 0.01\,\Omega \approx 0.67\,\text{W}$$

Since the resistor is rated for 3 W at 70°C, it provides sufficient power margin for the theoretical measurement range. Therefore, this resistor is suitable for motor current sensing because it provides low resistance, high power rating, good tolerance, low temperature drift, and reliable Kelvin connection capability.

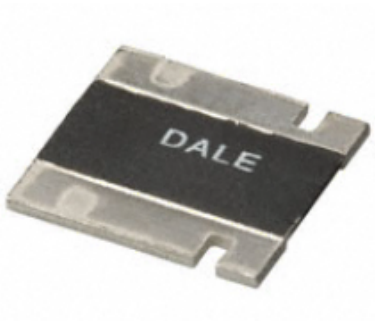


Figure 6: Vishay WSL3637R0100FEA current-sense resistor.

3.1.4 Power Supply Components

In this design, the main step-down converter is the **LMZ14201**. It generates the intermediate DCDC_5V rail from the input supply.

The main features considered for the LMZ14201 selection are listed as follows:

- Wide input voltage range from 6 V to 42 V
- Output voltage range from 0.8 V to 6 V
- Up to 1 A output current
- Integrated shielded inductor
- High efficiency operation
- Thermal shutdown and current limit protection
- Reduced external component count

This component was selected for three main reasons. First, it supports a wide input voltage range. Second, it can provide up to 1 A output current. Third, it integrates the power inductor inside the module, reducing the number of external components and simplifying the PCB layout.

Figure 7 shows the LMZ14201 package pinout and its simplified application schematic. The VIN pin is connected to the input supply, while the VOUT pin provides the regulated

output voltage. The FB pin is used for output voltage feedback, and the EN and RON pins are used for enable control and switching configuration. The integrated structure of the device makes it suitable for compact PCB implementation.

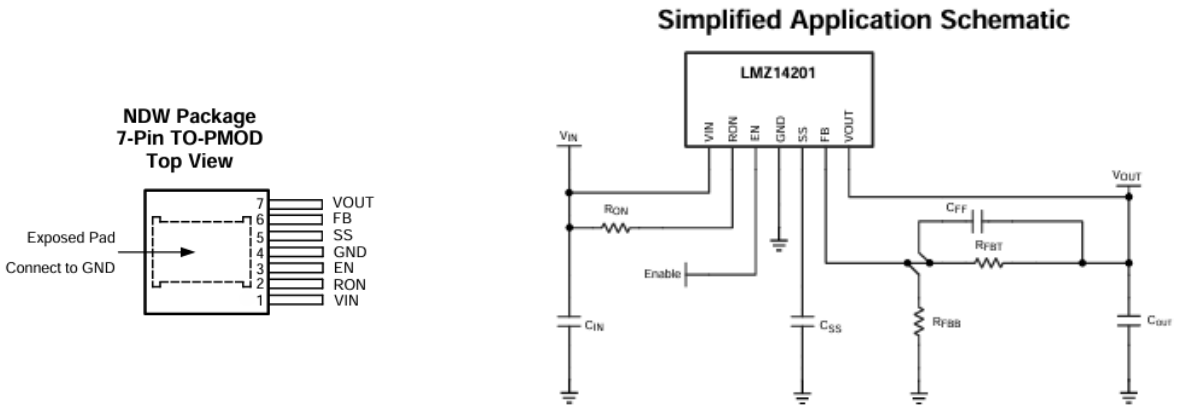


Figure 7: LMZ14201 package pinout and simplified application schematic.

After the DC-DC conversion stage, **TPS7A20** low-dropout regulators are used to generate clean low-voltage supply rails for sensitive circuits such as the INA226, the isolation interface, and the CC2640R2F. The LDO stage is useful because it reduces switching noise from the DC-DC converter and provides a more stable supply for measurement and RF circuits.

Figure 8 shows the typical TPS7A20 application schematic and package pinout. The IN pin receives the regulated input voltage, and the OUT pin provides the clean low-voltage supply rail. The EN pin allows the regulator to be enabled or disabled, while the input and output capacitors are used to ensure stable operation and reduce supply noise.

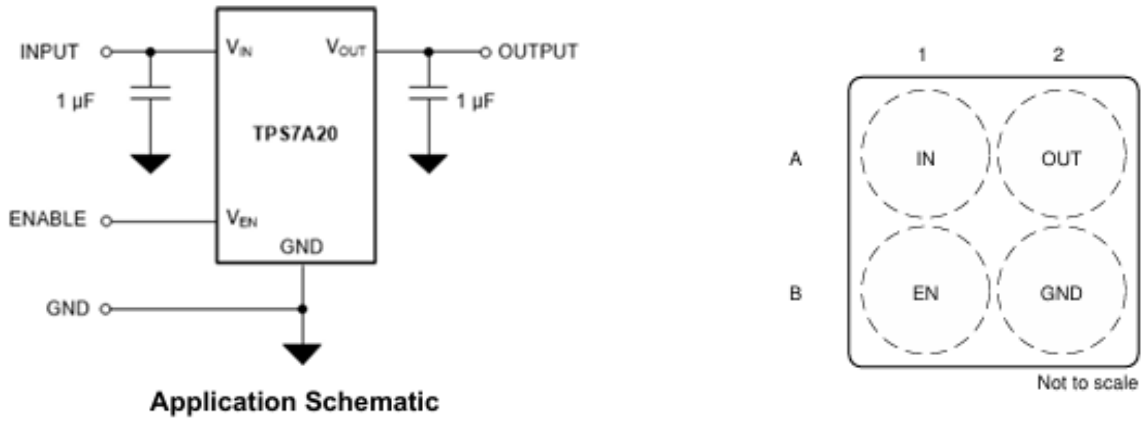


Figure 8: TPS7A20 application schematic and package pinout.

The main features considered for the TPS7A20 selection are listed as follows:

- Input voltage range from 1.6 V to 6.0 V
- Output voltage range from 0.8 V to 5.5 V

- Output current up to 300 mA
- Low output noise
- High power supply rejection ratio
- Low quiescent current
- Stable operation with small ceramic capacitors

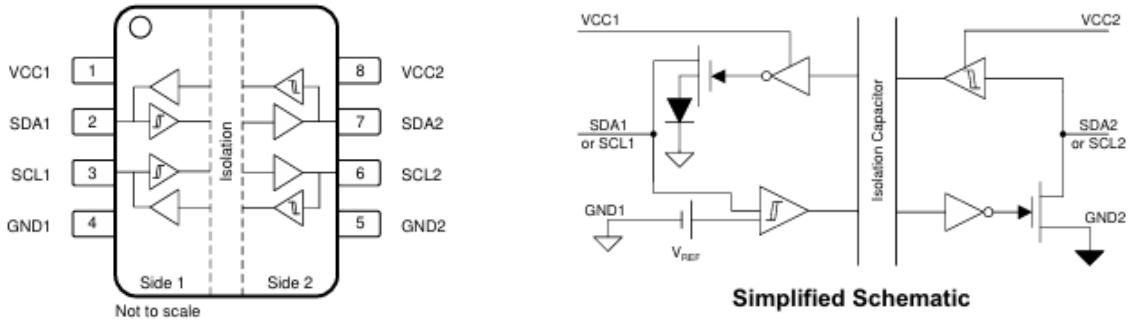
Overall, the combination of a DC-DC converter and LDO regulators provides both efficiency and low-noise power regulation. The LMZ14201 efficiently converts the input voltage to an intermediate rail, while the TPS7A20 regulators provide cleaner local supplies for the measurement, isolation, and BLE sections.

3.1.5 Isolation Components

The isolation section was included to separate the motor measurement side from the microcontroller and BLE communication side. Since the motor supply line can introduce noise, transients, and ground potential differences, electrical isolation improves the robustness and safety of the system.

In this design, the **ISO1540D** is used as the I^2C digital isolator. It isolates the SDA and SCL lines between the INA226 and the CC2640R2F while keeping the I^2C communication bidirectional. This is important because the INA226 sends the measured voltage, current, and power data to the microcontroller through the I^2C bus.

Figure 9 shows the pin configuration and simplified internal schematic of the ISO1540D. The device has two separated supply domains, where `VCC1` and `GND1` belong to Side 1, and `VCC2` and `GND2` belong to Side 2. The SDA and SCL lines are isolated through the internal isolation capacitor structure, allowing the I^2C signals to pass across the isolation barrier without a direct electrical connection between the two grounds.



(a) Pin configuration

(b) Simplified internal schematic

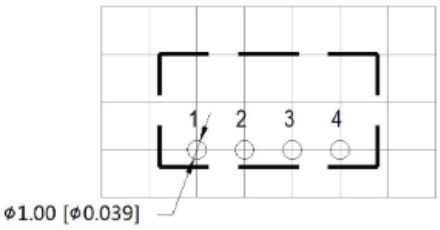
Figure 9: Pin configuration and simplified schematic of the ISO1540D I^2C digital isolator.

The main features considered for the ISO1540D selection are listed as follows:

- Bidirectional I^2C-compatible isolation
- Supports operation up to 1 MHz
- Supply voltage range from 3 V to 5.5 V
- Isolation rating of 2.5 kVrms for 1 minute
- High transient immunity
- Suitable for isolating the measurement interface from the control side

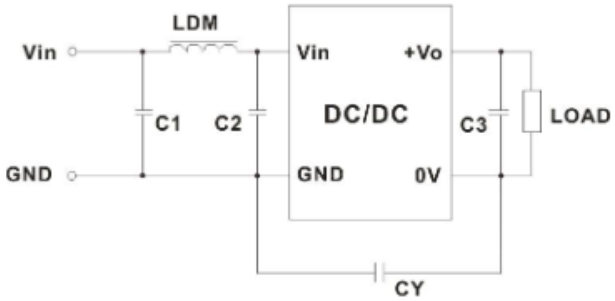
In addition to signal isolation, an isolated power supply is also required. For this purpose, the **B0505S-1WR3** isolated DC-DC converter is used. It converts a 5 V input into an isolated 5 V output, allowing the isolated measurement side to have its own floating supply.

Figure 10 shows the pin assignment and typical application circuit of the B0505S-1WR3. Pin 1 is connected to `GND`, Pin 2 is connected to `Vin`, Pin 3 is the isolated output ground `0V`, and Pin 4 provides the isolated positive output `+Vo`. In the typical application circuit, input capacitors are used to reduce input ripple, while the output capacitor helps stabilize the isolated output voltage. The isolation capacitor `CY` can be added between the primary and secondary sides to reduce common-mode noise.



Pin-Out	
Pin	Function
1	GND
2	Vin
3	0V
4	+Vo

(a) Pin assignment



(b) Typical application circuit

Figure 10: Pin assignment and typical application circuit of the B0505S-1WR3 isolated DC-DC converter.

The main features considered for the B0505S-1WR3 selection are listed as follows:

- 5 V input voltage

- Isolated 5 V output voltage
- 1 W output power
- Compact SIP package
- Isolation voltage up to 1.5 kVDC for 1 minute
- Operating temperature range from $-40°C$ to $+105°C$
- Suitable for isolated distributed power systems

The combination of the ISO1540D and the B0505S-1WR3 provides both signal isolation and power isolation. The ISO1540D isolates the I^2C communication path between the INA226 and the CC2640R2F, while the B0505S-1WR3 provides an isolated 5 V supply for the measurement side. This prevents disturbances from the motor side from directly affecting the microcontroller and BLE section, improving the reliability of the motor power analyzer.

3.2 Schematic Design

The schematic design follows the isolation concept of the system. The left side is the motor-side domain, which includes the motor input, protection circuit, shunt resistor, and INA226 measurement stage. The right side is the isolated microcontroller domain, which includes the CC2640R2F, BLE antenna, and supporting control circuits. This separation reduces the influence of motor-side noise, voltage transients, and ground disturbances on the low-voltage digital and wireless circuits. As shown later in Fig. 13, signal and power isolation are implemented between these two domains.

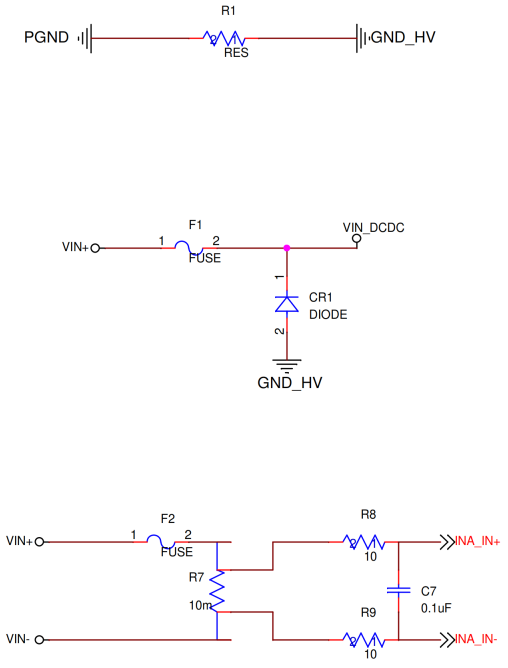


Figure 11: Power input protection and shunt sensing front-end circuit.

As shown in Fig. 11, this part of the schematic implements the motor power input protection and the current sensing front-end. The positive motor input `VIN+` first passes through fuse **F1** before generating the `VIN_DCDC` rail, which is used as the input supply for the following DC–DC conversion stage. A transient protection diode **CR1** is connected between `VIN_DCDC` and the high-voltage ground `GND_HV`. This device provides a discharge path for voltage spikes and helps protect the downstream power supply circuit from transient disturbances on the motor input line.

The lower part of the schematic shows the motor current measurement path. The motor current enters from `VIN+`, passes through fuse **F2**, and then flows through the 10 mΩ shunt resistor **R7** before returning to `VIN-`. The small voltage drop generated across **R7** is proportional to the motor current and is used as the differential sensing signal for the INA226. The two sensing nodes are routed to the measurement IC through `INA_IN+` and `INA_IN-`.

Resistors **R8** and **R9**, together with capacitor **C7**, form a differential low-pass input filter before the INA226 sensing pins. This filter attenuates high-frequency noise generated by motor switching or cable parasitics, improving the stability of the shunt voltage measurement. In addition, resistor **R1** provides a controlled connection between `PGND` and `GND_HV`, allowing the ground reference strategy of the high-voltage input section to be defined in the schematic while keeping the power and sensing return paths clearly separated.

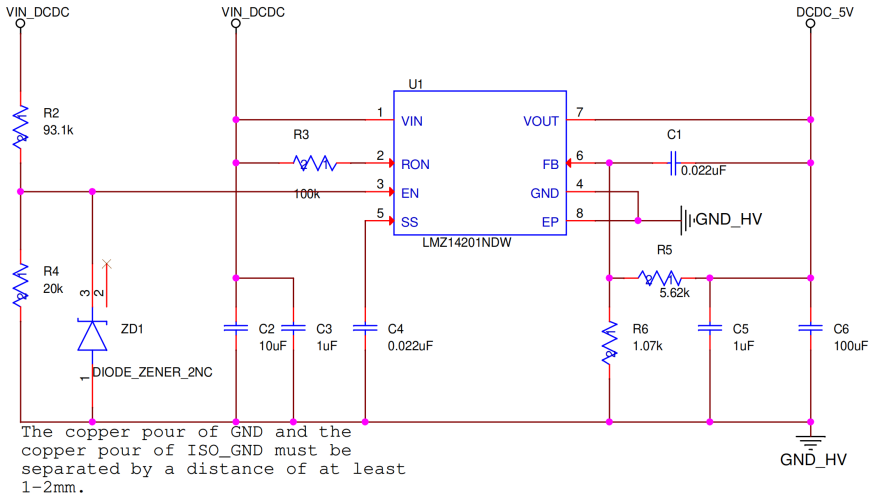


Figure 12: DC–DC conversion circuit for generating the 5 V supply rail.

Fig. 12 shows the DC–DC conversion stage that generates the intermediate `DCDC_5V` rail from `VIN_DCDC`. The main device is the **LMZ14201NDW**. The input capacitors **C2** and **C3** reduce input ripple, **R3** and **C4** configure the switching and soft-start behavior, and the feedback divider formed by **R5** and **R6** sets the output voltage. The output capacitors **C5** and **C6** provide basic filtering for the 5 V rail.

Although the DC–DC converter is efficient and suitable for stepping down the motor input voltage, its switching operation can introduce ripple, spikes, and high-frequency noise on

the output rail. These disturbances are not ideal for sensitive circuits such as the INA226 measurement front-end, the I^2C isolation interface, and the BLE microcontroller supply. Therefore, the `DCDC_5V` rail is treated as an intermediate supply rather than the final clean supply. In the following stage, LDO regulators are used to further filter this rail and generate cleaner low-voltage supplies for the analog measurement and digital control circuits.

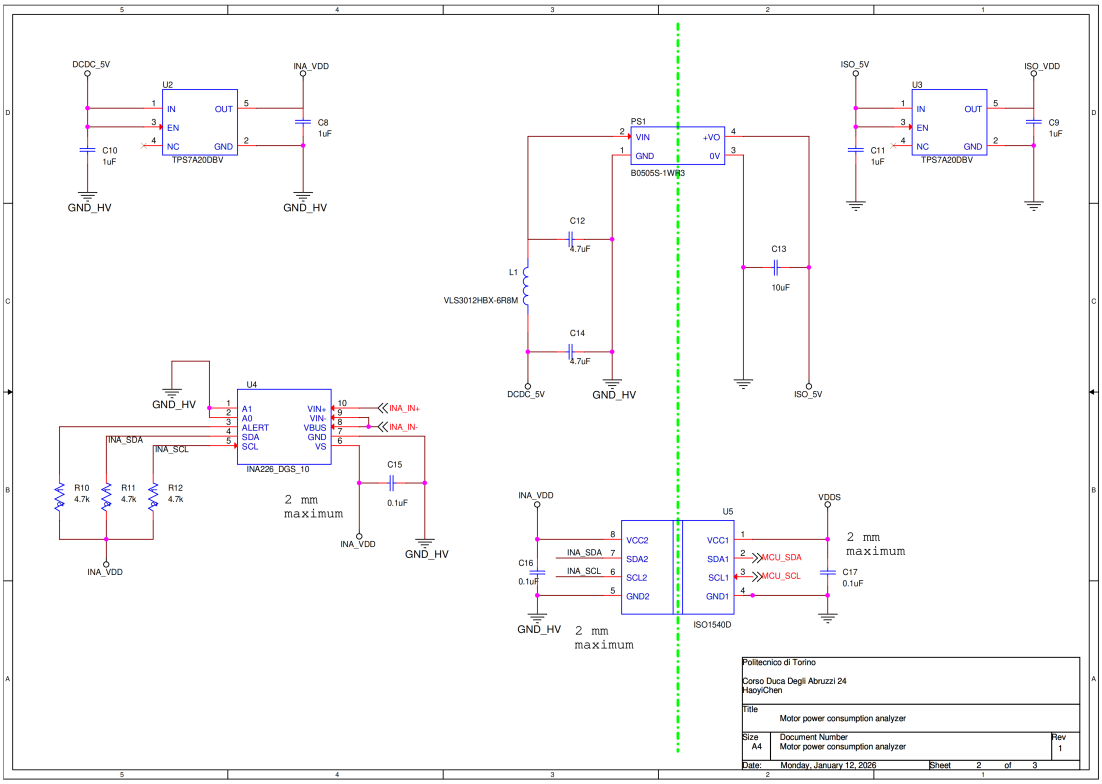


Figure 13: INA226 measurement circuit, isolated power supply, and I^2C isolation circuit.

Fig. 13 shows the measurement and isolation section of the schematic. The green dashed line marks the isolation boundary: the left side is the motor-side measurement domain referenced to `GND_HV`, while the right side belongs to the isolated microcontroller domain. This structure keeps the noisy motor power side separated from the low-voltage control and BLE circuits.

On the motor side, the `DCDC_5V` rail is regulated by the TPS7A20 LDO **U2** to generate `INA_VDD` for the INA226 **U4**. This LDO stage is important because the previous DC–DC converter may still produce ripple and high-frequency spikes. A cleaner supply helps improve the stability of the INA226, which measures the small differential shunt voltage through `INA_IN+` and `INA_IN-`, as well as the motor bus voltage through `VBUS`.

Power isolation is implemented by the B0505S isolated DC–DC module **PS1**. It converts the motor-side `DCDC_5V` into an isolated `ISO_5V` rail with a separated ground reference. After that, another TPS7A20 LDO **U3** generates `ISO_VDD`, providing a cleaner supply for the isolated interface circuitry. The surrounding capacitors and inductor are used to stabilize the isolated supply and reduce conducted noise.

Signal isolation is provided by the ISO1540D **U5**. The INA226 communicates on the motor side using `INA_SDA` and `INA_SCL`, while the isolated side outputs `MCU_SDA` and `MCU_SCL` to the CC2640R2F. In this way, the I^2C data can cross the isolation barrier without directly connecting the two ground domains. Overall, this page combines clean local regulation, voltage and current measurement, isolated power, and isolated digital communication.

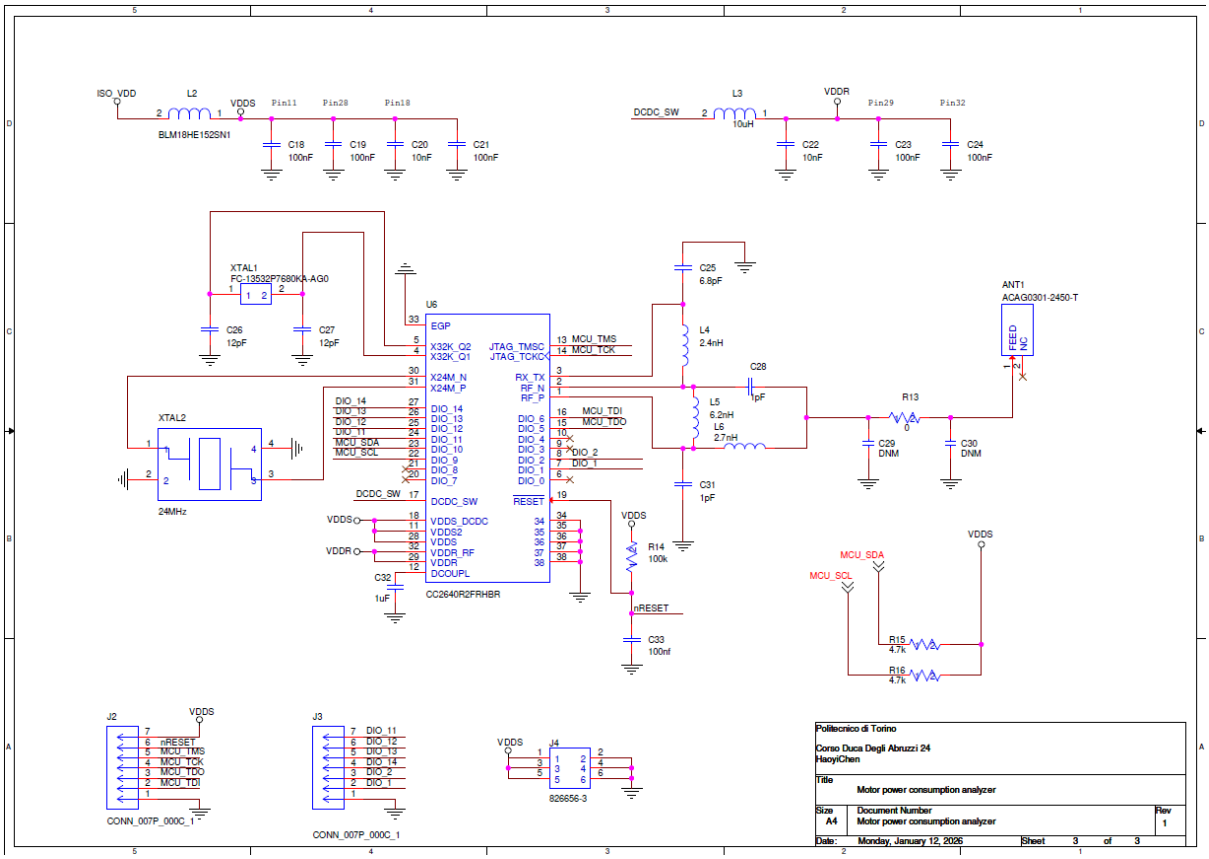


Figure 14: CC2640R2F microcontroller, BLE RF circuit, clock circuit, and programming interface.

As shown in Fig. 14, the CC2640R2F is used as the main microcontroller and BLE communication device. The isolated I^2C signals are connected to the microcontroller through `MCU_SDA` and `MCU_SCL`. The CC2640R2F reads the voltage, current, and power data from the INA226 and then transmits the processed measurement results through BLE. The schematic also includes the required crystal circuits, reset circuit, RF matching network, antenna connection, and JTAG/debug interface. These parts allow the microcontroller to operate correctly, communicate wirelessly, and be programmed or debugged during development.

Overall, the schematic design follows a modular structure. The first stage provides protected power input and current sensing, the second stage performs voltage and current measurement with electrical isolation, and the third stage processes the digital data and sends it wirelessly through BLE. This design makes the motor power analyzer suitable for real-time monitoring of motor voltage, current, power, and energy consumption.

3.3 Layout Design

The system features a highly optimized 4-layer PCB layout specifically tailored for high-voltage, high-current diagnostic applications. To preserve signal integrity, maximize thermal dissipation, and optimize RF performance, a strict functional zoning and isolation routing strategy were executed across a standardized JLCPCB 7628 stack-up structure, balancing manufacturing efficiency with strict impedance requirements.

3.3.1 4-Layer Stack-up and Layer Assignment

The layout utilizes the industry-standard JLCPCB 4-layer 7628 stack-up structure with a total nominal thickness of 1.6mm. The physical layers are assigned systematically to maximize high-frequency noise shielding and accommodate heavy motor switching currents, the integrated configuration of which is visualized in Figure 15.

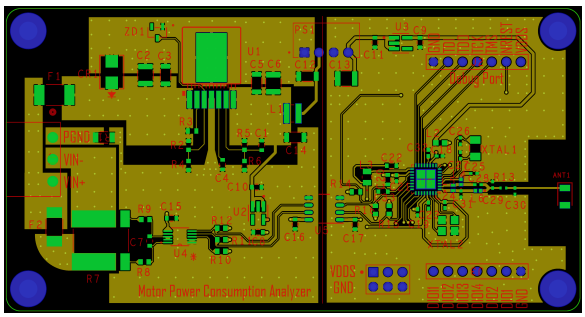
Layer	Material Type	Thickness	
Top Layer	Copper	0.035mm	
Prepreg	7628*1	0.21040mm	
Inner Layer L2	Copper	0.0152mm	1.1mm H/HOZ with copper
Core	Core	1.065mm	
Inner Layer L3	Copper	0.0152mm	
Prepreg	7628*1	0.21040mm	
Bottom Layer	Copper	0.035mm	

Figure 15: Detailed physical parameters and material specifications of the JLCPCB 4-layer 7628 PCB stack-up.

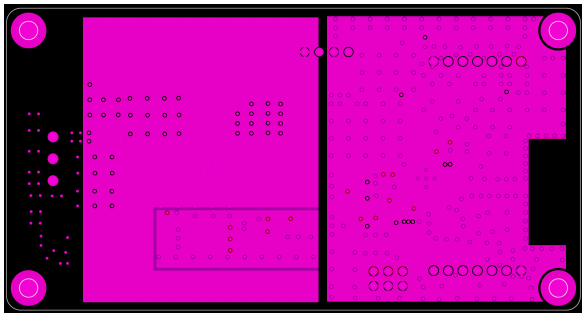
The functional assignment of the copper layers follows a rigid hierarchical topology to isolate critical signal domains. Layer 1, the Top Layer, serves as the primary routing and component placement layer. To eliminate unnecessary via transitions and minimize parasitic inductance, all components are placed entirely on this layer, and the vast majority of signal traces are routed here. Furthermore, it hosts the high-current input power distribution via localized heavy copper pours (VCC_IN, 5V) and critical RF antenna routing, featuring an outer copper thickness of 1oz (35μm) as visualized in Figure 16a.

Immediately beneath, Layer 2 (Inner 1) is configured as a solid 0.5oz (17.1μm) ground plane, serving as the primary high-speed return path shown in Figure 16b. This plane is physically split underneath the central isolation barrier to separate the raw power ground (`PGND`) from the isolated digital ground (`GND`). Layer 3 (Inner 2) acts as a secondary solid 0.5oz ground plane dedicated to electromagnetic interference (EMI) shielding, as depicted in Figure 16c. This dual-GND structure formed by Layer 2 and Layer 3 provides exceptional shielding, preventing high-frequency switching noise from cross-coupling into sensitive routing regions.

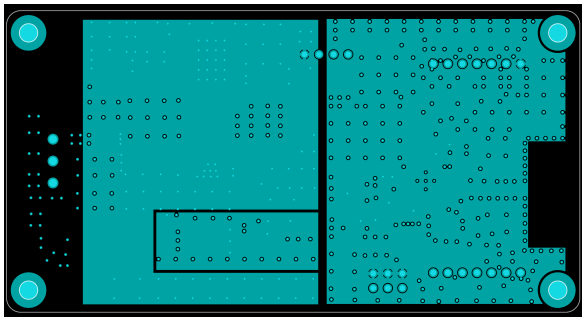
Finally, Layer 4, the Bottom Layer, is dedicated primarily to auxiliary routing and shielding with a thickness of 1oz (35μm), as illustrated in Figure 16d. It contains only a few low-speed signal traces on the MCU side, while its remaining area is covered by large ground copper pours and symmetrical power planes that mirror the Top layer topology.



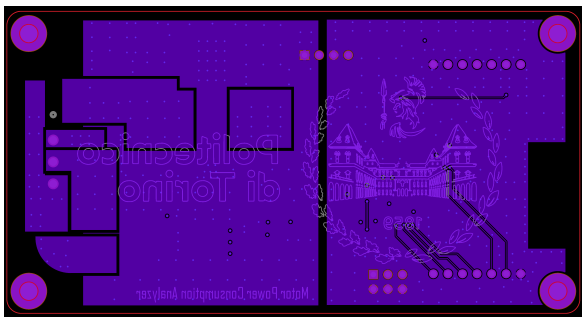
(a) Top Layer (High-current copper pours and component placement)



(b) Layer 2 (Inner GND plane with vertical isolation split)



(c) Layer 3 (Secondary Inner GND plane for EMI shielding)



(d) Bottom Layer (Low-speed signal traces and auxiliary routing)

Figure 16: 4-Layer PCB routing and functional isolation boundaries of the Motor Power Consumption Analyzer.

3.3.2 Functional Zoning and Sub-system Distribution

To achieve maximum noise immunity and structural coherence, the geometric topology of the Top layer is strictly compartmentalized into distinct sub-sections based on operational voltage and signal sensitivity. The spatial distribution of these components and their respective ground domains are comprehensively partitioned into six core functional regions, as highlighted in Figure 17.

Region 1 demarcates the primary External Power Input stage, which is equipped with low-impedance screw terminals to securely interface with the 8–36V raw motor voltage source. This input port is guarded by onboard fuses (F1 and F2) and a transient voltage suppressor to intercept overcurrent conditions and high-voltage inductive spikes right at the boundary before they propagate into the downstream circuitry.

Directly adjacent, Region 2 encloses the DC-DC Buck Converter along with its critical peripheral components. The switching regular circuitry, including the power inductor and the high-frequency input/output ceramic capacitors, is tightly grouped to minimize the geometric area of the high di/dt switching loop. To manage heavy switching currents and minimize parasitic trace inductance, wide copper polygons are poured symmetrically on both the Top and Bottom layers for the main power paths. These overlapping power tracks are subsequently stitched together with a high density of stitching vias, which drastically lowers DC resistance, reduces localized voltage drops, and enhances thermal dissipation by converting the inner ground planes into structural heat sinks.

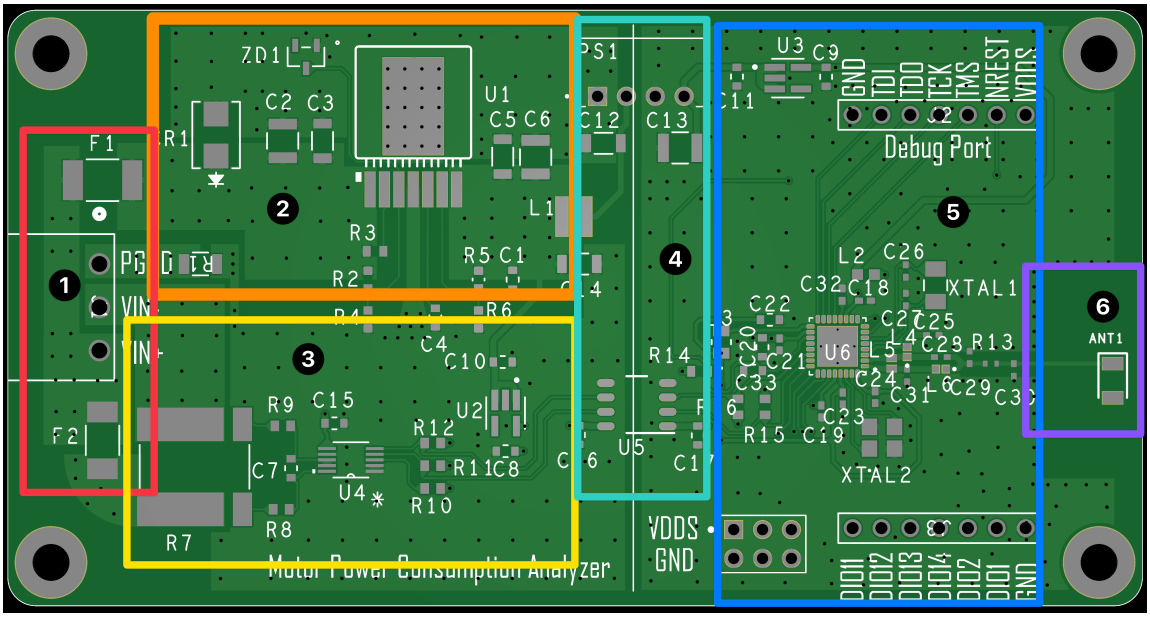


Figure 17: Functional zoning and component distribution on the Top layer of the Motor Power Consumption Analyzer.

Region 3 encompasses the high-precision analog sensing block, hosting the INA226 current-shunt monitor and the low-temperature-coefficient shunt resistor (R7/R8). To overcome trace-resistance-induced voltage drops and eliminate measurement offsets, the shunt resistor is strictly routed using a 4-wire Kelvin connection. The differential trace pair is routed symmetrically and tightly coupled on the Top layer, referencing the solid Power Ground (`PGND`) loop to ensure that the 16-bit ADC acquires an ultra-stable voltage differential free from ground displacement errors.

Region 4 acts as the central Physical Isolation Bridge, completely bisecting the PCB ground system into two independent electrical domains separated by a vertical 1.5mm clearance barrier. This critical boundary interfaces the high-power domain with the processing domain exclusively through specialized component footprints to sever direct galvanic paths. Power isolation across the split is achieved via a B0505S isolated DC-DC module, which steps down and cross-feeds power from the left side to the right side to establish an independent supply network. In parallel, bidirectional signal isolation is maintained by the ISO1540D digital isolator, which sits directly astride the split line to pass I2C communication lines (SCL/SDA) via capacitive coupling. This unified bridging strategy effectively prevents high-frequency digital switching noise and motor ground loops from cross-coupling between the decoupled sub-systems.

Region 5 defines the Isolated Control Zone, which functions as an electrically quiet sanctuary for the core processing unit. It contains the CC2640R2F wireless MCU, its external tuning crystals, and a dedicated debugging port, all referencing a fully decoupled, continuous Digital Ground (`GND`) plane.

Finally, Region 6 encloses the Bluetooth Antenna (`ANT1`) module. Driven by the specific dielectric properties of the JLC 7628 prepreg layer, which provides a precise Top-to-Layer2 thickness of 0.2104mm and a nominal dielectric constant (ε_r) of 4.4, the RF trace connecting the MCU to the antenna footprint was precisely calculated and routed

with a specific line width of 14.1mil. This optimized geometric footprint establishes a highly stable 50Ω characteristic impedance, minimizing signal reflection and maximizing wireless transmission range to the mobile application. Crucially, a π-type impedance matching network consisting of three passive footprints (L2, C26, and C32) is reserved immediately preceding the antenna input. This matching network serves as a hardware safeguard, granting full tunability to compensate for unexpected parasitic impedance or signal degradation induced by the external metallic enclosure, thereby ensuring reliable wireless link quality during field deployment. From a manufacturing perspective, all traces, clearances, and via dimensions across these regions were kept well within standard production capabilities, maintained at a minimum trace width/spacing greater than 6mil and a minimum via hole diameter of 0.3mm to guarantee optimal fabrication yields.

4 Manufacturing and DFM Validation

Following the completion of the physical layout within the Cadence Allegro environment, the design was translated into professional fabrication datasets. The copper layers, solder masks, and silkscreens were exported as standardized artwork files (`.art` in RS-274X format), including `TOP.art`, `BOTTOM.art`, `GND.art`, and `POWER.art`. Concurrently, the NC drill files (`.drl`) and an IPC-standard netlist (`.ipc`) were generated to provide a complete manufacturing package.

The physical parameters of this layout were constrained by a custom set of Design Rules tailored to the academic project requirements. To verify that these academic constraints align with realistic industrial tolerances, the complete Gerber archive was submitted to the manufacturer, JLCPCB, for an automated Design for Manufacturing (DFM) pre-review.

The manufacturer's system performed an automated integrity check. The design successfully cleared all production rules (Figure 18) and advanced directly to the fabrication line, where the progression was monitored through real-time milestone tracking (Figure 19).

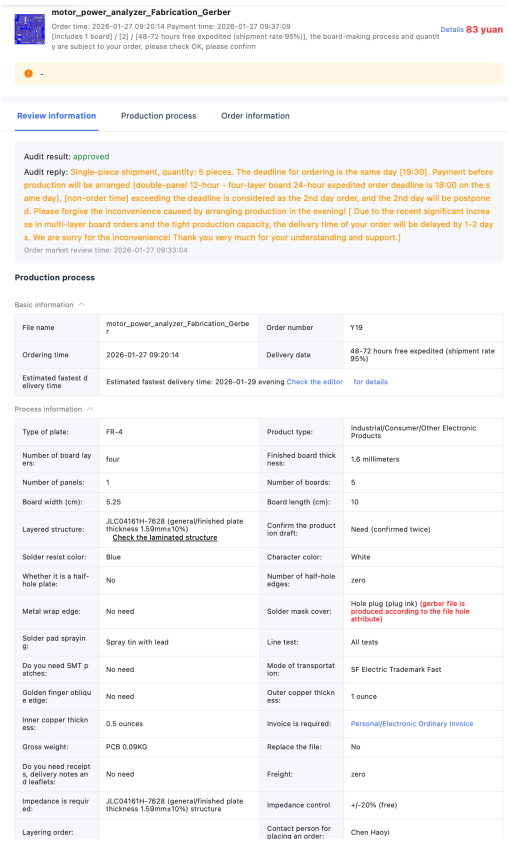


Figure 18: Manufacture approved.

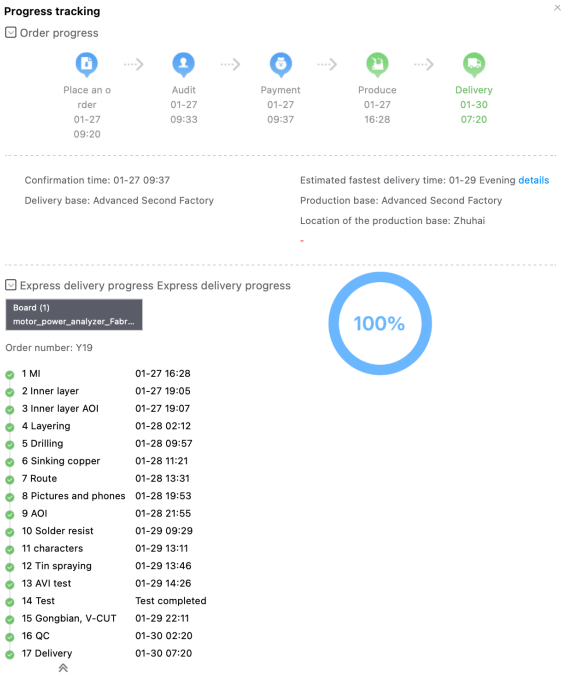


Figure 19: Real-time fabrication tracking.

5 Hardware Testing

Following the successful fabrication of the 4-layer PCB by JLCPCB, a systematic hardware bring-up and verification procedure was initiated to validate the electrical integrity and functional soundness of the physical prototype. This phase serves as a critical bridge between theoretical circuit design and high-level software deployment, ensuring that all sub-systems operate within their nominal electrical boundaries before full system integration.

The component assembly process was executed manually using a combination of a high-precision hot-air rework station for surface-mount technology (SMT) integrated circuits, such as the CC2640R2F wireless MCU and the ISO1540D digital isolator and a temperature-controlled soldering iron for larger passive components, connectors, and protection terminals. Special attention was paid to the thermal profiling during the manual reflow of the central isolation components and the shunt network to prevent thermal damage to the micro-elements. The completely assembled top-side physical prototype of the Motor Power Consumption Analyzer is comprehensively illustrated in Figure 20. The bottom-side layout design is presented distinctly in Figure 21.

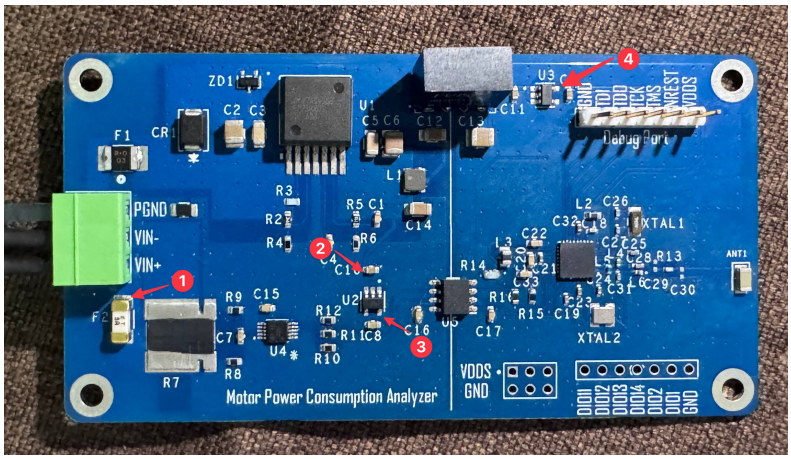


Figure 20: Fully assembled PCB prototype top layer with sequential power rail test nodes.



Figure 21: Fully assembled PCB prototype bottom layer.

Immediately following the visual inspection under a magnifying lens to ensure the absence of solder bridges or cold joints, a sequential power-on testing methodology was implemented to verify the structural integrity of the localized power distribution networks. Rather than powering the entire board simultaneously, voltage propagation was validated stage-by-stage across the critical supply path nodes as sequentially superimposed in Figure 20.

Node 1 highlights the External Power Input stage where a regulated DC laboratory power supply was connected via the screw terminals to inject a nominal input voltage within the 8–36V range. Upon verifying that the total quiescent current draw remained well within the micro-ampere spectrum, the switching state of the DC-DC Buck Converter was examined at Node 2, which successfully confirmed a stable, low-ripple step-down output of precisely 5.02V under no-load conditions. Finally, the downstream regulation paths were verified at Node 3, which encompasses the output terminals of the two independent linear regulators (LDOs). The multimeters recorded a steady voltage of 3.31V on both the primary power side and the isolated control side, demonstrating that the B0505S isolation transformer and the low-dropout regulators were functioning optimally. These empirical measurements conclusively demonstrate that the power distribution topology, the cross-isolation bridge, and the localized copper rails suffer from no short-circuits or catastrophic voltage drops, establishing a thoroughly verified and secure electrical foundation for the subsequent MCU firmware debugging and analog sensing calibration.

6 Software Design

The software of the motor power analyzer was designed as a periodic measurement and BLE transmission framework. The main functions of the firmware are to initialize the system peripherals, configure the INA226 current and power monitor, read the motor electrical parameters, determine whether the motor current is detected, and transmit the measurement data through BLE.

6.1 Firmware Architecture

The firmware is based on the Texas Instruments BLE 5.0 Simple Peripheral project for the CC2640R2F microcontroller. It is developed in Code Composer Studio using the SimpleLink CC2640R2 SDK and runs on TI-RTOS. The software structure follows a two-layer organization: the BLE protocol stack is compiled as a stack library, while the application project contains the motor analyzer firmware, board configuration, INA226 measurement functions, and BLE application logic.

At system start-up, the entry point initializes the TI-RTOS environment, the ICall layer, and the board peripherals. The ICall layer acts as the communication bridge between the application task and the BLE stack, so the application does not access the BLE stack directly. Instead, BLE events, GATT operations, and connection state changes are delivered to the application through the event-driven task mechanism. The main application task is implemented as a periodic event loop, which handles BLE activity, timer events, and motor measurement updates.

The firmware supports the custom motor analyzer PCB through a dedicated board support package. The board files define the pin mapping, peripheral configuration, and driver tables for the `MOTOR_ANALYZER` hardware. This is important because the custom PCB uses the CC2640R2F in a different package and pin assignment from the standard TI LaunchPad. Through this board layer, the same application logic can access the correct I^2C pins, GPIOs, and debugging interface used in the hardware design.

6.2 Software Logic

The software logic of the BLE firmware is shown in Fig. 22. After power-on, the CC2640R2F initializes the board drivers, I^2C interface, INA226 configuration, BLE stack, and application task. Once initialization is complete, the device starts BLE advertising and waits for a mobile phone or computer to connect as a BLE central device.

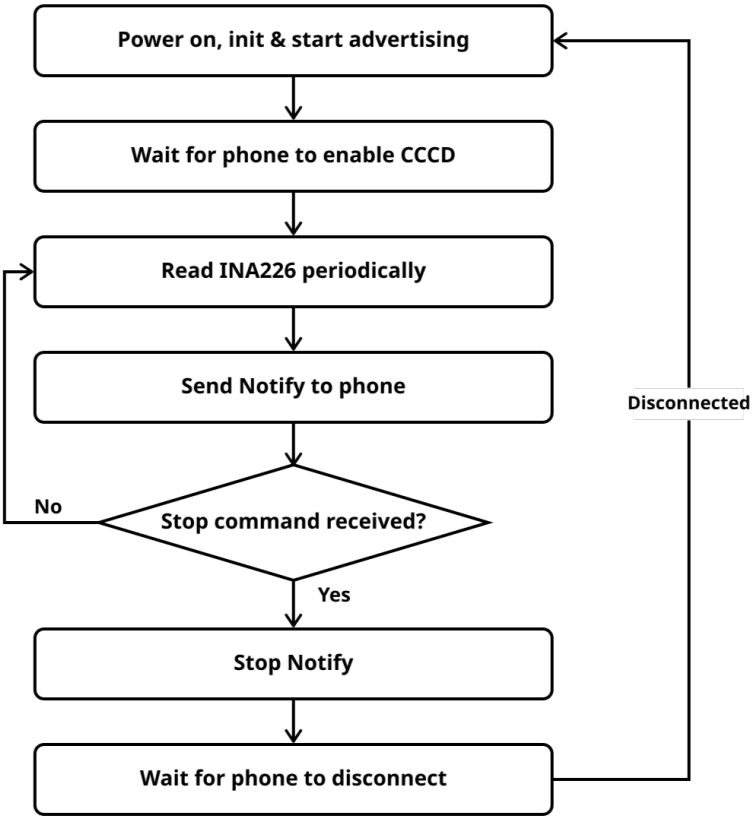


Figure 22: BLE firmware logic of the motor power analyzer.

After a BLE connection is established, the firmware waits for the client to enable notification through the Client Characteristic Configuration Descriptor (CCCD). This step is necessary because the analyzer should only send periodic measurement data when the user application is ready to receive it. If notification is not enabled, the firmware remains connected but does not continuously transmit data.

When notification is enabled, the firmware enters the active measurement loop. In each cycle, the CC2640R2F reads the INA226 through the isolated I^2C bus and obtains the motor current, bus voltage, and power values. The raw register data are converted into physical units according to the INA226 calibration settings. The processed values are then written to the custom BLE GATT characteristics and sent to the connected client by notification.

The loop continues while the BLE connection remains active and the client keeps notification enabled. If the user sends a stop command or disables notification, the firmware stops periodic data transmission and waits for the next command or connection event. If the BLE connection is disconnected, the device returns to the advertising state so that another client can connect again. This logic allows the motor power analyzer to operate as a low-power BLE peripheral while still providing real-time measurement updates when required.

6.3 Mobile Application Interface

The mobile application provides the user interface for receiving and displaying the BLE measurement data from the motor power analyzer. As shown in Fig. 23, the application presents the three main electrical parameters of the motor: load current, load voltage, and load power. These values correspond to the data measured by the INA226 and transmitted by the CC2640R2F through the custom BLE GATT characteristics.

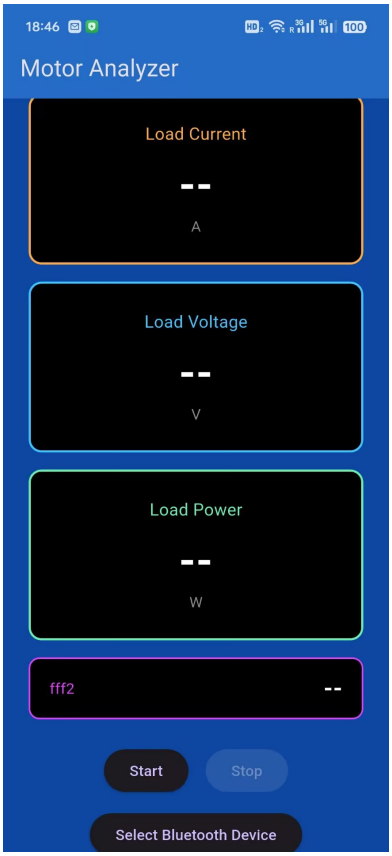


Figure 23: Mobile application interface for motor power monitoring.

The interface was developed using Flutter, and the current version was compiled only for the Android platform. It contains a Bluetooth device selection button, which allows the user to search for and connect to the motor analyzer peripheral. After the BLE connection is established, the user can press the start button to enable measurement notification. The current, voltage, and power display cards are then updated when new data are received from the firmware. The stop button is used to disable the measurement update process. This application interface makes the system easier to use because the measured motor power information can be observed directly on a mobile device without additional laboratory instruments.

7 Full Functional Validation

This chapter presents the functional validation of the motor power consumption analyzer after the hardware and firmware integration. The purpose of the test was to verify whether the complete system could measure the motor-side electrical parameters and transmit the results to the mobile application through BLE.

7.1 System-Level Test Result

The integrated test setup is shown in Fig. 24. In this validation, a power resistor was used as a representative load to simulate the motor load. The motor analyzer PCB was connected to an external DC power supply and the resistor load, while the mobile application was connected to the CC2640R2F through BLE and displayed the received load current, load voltage, and load power values in real time.

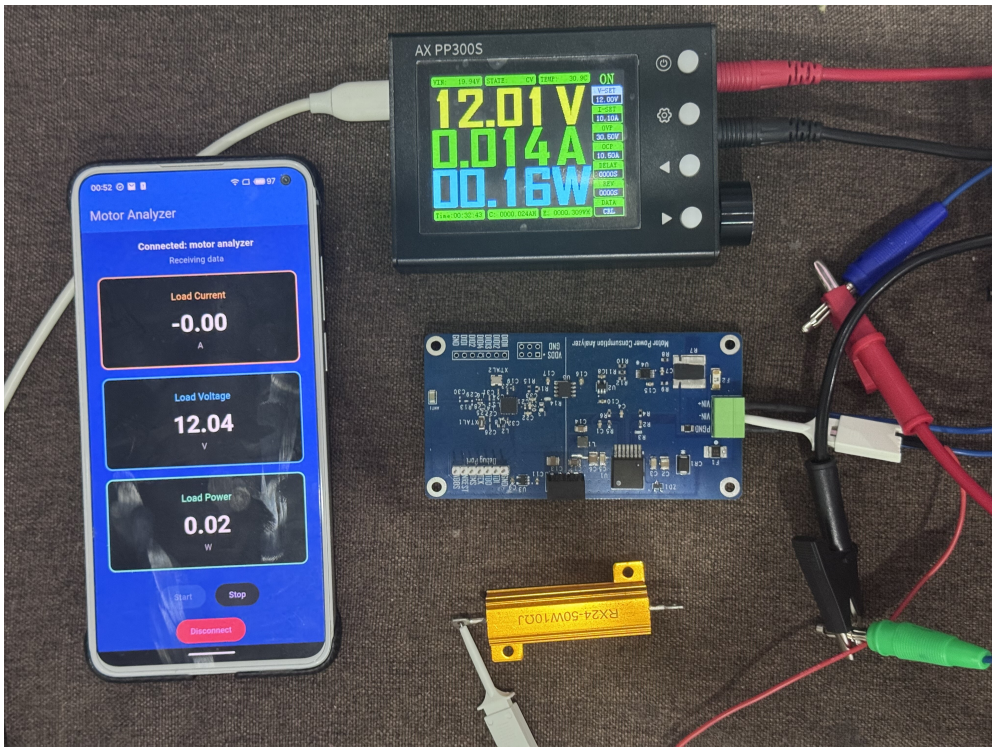


Figure 24: Functional validation result of the motor power analyzer.

During the resistor-load test, the voltage measurement result was correct. The external power supply showed approximately 12.01 V, while the mobile application displayed approximately 12.04 V. This small difference is acceptable for the initial functional validation and confirms that the bus voltage measurement path of the INA226 was working. More importantly, it also confirms that the BLE communication link, the CC2640R2F firmware, the mobile application, and the I^2C readout process were functioning correctly, because the voltage value had to be read from the INA226 and then transmitted through BLE before being displayed on the phone.

However, the measured current and power values were not correct. The test condition

used a 12 V supply and a 10 Ω resistor load. Therefore, when the other terminal of the resistor load was connected into the circuit, the theoretical load current should have been approximately 1 A. Nevertheless, the current value displayed by the mobile application still remained close to zero. This connection step is not fully shown in Fig. 24, but it can be observed in the last one and a half minutes of the recorded test video. The displayed power value was therefore also incorrect. This behavior is consistent with the working principle of the INA226: the power value is calculated based on the measured current and bus voltage. Therefore, if the current measurement is incorrect, the calculated power value will also become incorrect even when the voltage measurement is normal.

7.2 Fault Analysis and Debugging Process

The debugging process was carried out step by step to separate possible firmware, communication, and hardware causes. First, since the voltage value was correctly displayed on the mobile application, the BLE data transmission could be considered valid. The CC2640R2F was able to send measurement data to the phone, and the phone application was able to receive and display the data. In addition, because the voltage value was read from the INA226 through the I^2C interface, the CC2640R2F I^2C driver and the isolated I^2C communication path were also verified to be working.

After confirming that the communication path was functional, the debugging focused on the current measurement path. The INA226 calculates current from the shunt voltage measured between the `VIN+` and `VIN-` pins. Therefore, the shunt voltage register was read directly during debugging. The result showed that the shunt voltage value remained at zero. This indicates that the INA226 did not detect a valid differential voltage across the shunt resistor, even though the system input voltage could still be measured correctly.

Based on this observation, the most likely cause is located at the hardware level rather than in the BLE firmware or application software. Possible causes include an issue with the INA226 device itself, an incorrect or weak connection between the shunt resistor and the INA226 sense pins, a problem in the Kelvin sensing path, or an error in the surrounding current-sensing circuit design. Since the bus voltage measurement was normal while the shunt voltage remained zero, the failure is specifically related to the current-sensing part of the INA226 circuit instead of the complete digital communication chain.